AIAA JOURNAL
Vol. 48, No. 3, March 2010

Physics and Regimes of Supersonic Combustion

Antonella Ingenito* and Claudio Bruno†
University of Rome "La Sapienza," 00184 Rome, Italy

DOI: 10.2514/1.43652

Understanding the physics of supersonic combustion is the key to design a performing engine for scramjet-powered vehicles. Despite studies on supersonic combustion dating back to the 1950s, there are still numerous uncertainties and misunderstandings on this topic. The following questions need to be answered: How does compressibility affect mixing, flame anchoring, and combustion efficiency? How long must a combustor be to ensure complete mixing and combustion while avoiding prohibitive performance losses? How can reacting turbulent and compressible flows be modeled? Experimental results in the past have shown that supersonic combustion of hydrogen and air is feasible and takes place in a reasonable distance, which is a necessary requirement in actual hypersonic vehicles powered by supersonic combustion ramjets. These results are explained based on a theoretical analysis of the physical mechanisms driving mixing and combustion in supersonic airstreams, where they are found to be different from those in the incompressible regime. In particular, the classic Kolmogorov scaling is shown to be no longer strictly valid, and the flame regime is predicted to be significantly affected by compressibility and different from that of subsonic flames. This analysis is also supported by the results of the numerical simulations presented, showing that by generating sufficiently intense turbulence, a supersonic combustion flame is short and can indeed anchor within a small distance from fuel injectors, with the flame typically burning in the so-called flamelets-in-eddies regime.

Nomenclature

A	=	Arrhenius rate preexponential
a	=	speed of sound
B	=	baroclinic term within the vorticity equation
conv	=	convective term in the vorticity equation
CP	=	dilatational term in the vorticity equation
c_p	=	heat capacity at constant pressure
CV	=	diffusive term due to density gradients and viscous stresses coupling within the vorticity equation
D	=	drag
Da	=	Damköhler number
DV	=	diffusive term due to coupling between strain rate and viscous gradients in the vorticity equation
D_{ij}	=	binary diffusivity coefficient in a mixture
diff	=	diffusive term due to viscous gradients in the vorticity equation
E	=	turbulent kinetic energy per unit wave number
$\bar{E}$	=	strain rate tensor
E_A	=	activation energy
F	=	thrust
f_i	=	volume force applied to the ith species
H	=	helicity
h_{fi}	=	enthalpy of formation of the ith species
h_i	=	sensible enthalpy of the ith species
I	=	inertial term in the vorticity equation
L_0	=	integral turbulence scale
l_k	=	dissipative scale
l_m	=	turbulent characteristic scale length
k	=	wave number
k_s	=	$Ma_{\text{sub}}/Ma_{\text{sup}}$
M	=	molecular weight
Ma	=	Mach number
Ma_s	=	small scale Mach number
Ma_{sub}	=	transversal Mach (subsonic)
Ma_{sup}	=	streamwise Mach (supersonic)
m	=	molecular mass
N	=	number of chemical species
N_A	=	Avogadro number
n	=	number of moles
p	=	pressure
$\Re$	=	universal gas constant
Re	=	Reynolds number
S_l	=	laminar flame speed.
T	=	temperature
t_d	=	mixing time
t_k	=	kinetics time
t_r	=	residence time
U	=	streamwise velocity
$\bar{u}$	=	velocity vector with components (u, v, w)
u'	=	velocity fluctuation
V	=	cell volume
V^*	=	turbulent structure volume
VS	=	vortex stretching in the vorticity equation
VV	=	diffusive term due to viscous stresses and velocity gradients coupling in the vorticity equation
V_{air}	=	air speed
$\bar{V}_i$	=	diffusion velocity of the ith species
v'	=	eddy turnover velocity
$[X]$	=	X species concentration
X, Y	=	generic molecular species
x	=	distance from the injectors
$\bar{x}$	=	position vector of components (x, y, z)
$[Y]$	=	Y molecular concentration
Y_k	=	mass fraction of the kth species
z_V	=	collisional frequency per unit volume
α	=	thermal diffusivity
γ	=	heat capacity ratio (c_p/c_v)
γ^*	=	fraction of the cell volume occupied by subgrid fine structures
δ_l	=	flame thickness
ε	=	rate of turbulent kinetic energy dissipation per unit volume
η_c	=	combustion efficiency

Presented as Paper 812 at the 47th AIAA Aerospace Sciences Meeting, Orlando, FL, 1 May–1 August 2009; received 5 February 2009; revision received 29 May 2009; accepted for publication 10 September 2009.

*Ph.D. Graduate, Department of Mechanics and Aeronautics, Via Eudossiana 18.

†Professor. Department of Mechanics and Aeronautics, Via Eudossiana 18. Associate Fellow AIAA.

μ = dynamic viscosity
ν = kinematic viscosity
ρ = density
$\bar{\bar{\sigma}}$ = stress tensor
σ = collisional cross section
Φ = energy dissipation function
$\dot{\omega}$ = reaction rate
$\bar{\omega}$ = vorticity vector with components $(\omega_x, \omega_y, \omega_z)$
$\tilde{}$ = large-eddy-simulation filtered value of the quantity

Subscripts

i = ith vector component
j = jth vector component
k = index of the kth species
l = index of the lth species
N = large-eddy-simulation corrected value of the quantity
0 = equilibrium or reference value

Superscript

$*$ = large-eddy-simulation subgrid value of the quantity

I. Introduction

IN ADDITION to the personal interest by these authors, supersonic combustion (SC) and supersonic combustion ramjets (SCRJ) are potentially very important for future launchers and hypersonic cruisers. In this context, the goal of this paper is to present and discuss the physics and modeling of SC necessary to simulate turbulent mixing and combustion in SCRJ [1]. (A review of *nonreacting* hypersonic turbulence modeling is in [2].) Computational fluid dynamics (CFD) plays a growing role in SC research, but these authors feel that its physics are still partially understood and thus need at least the same attention as that devoted to accuracy and consistency of numerical schemes. In fact, the physics of compressible and reacting flows seem in recent years to have taken a back seat to numerics.

SC is not a new topic; it goes back to the conclusion reached by Ferri [3] that with increasing flight Mach numbers, the airflow through airbreathing engines must eventually remain supersonic. Public information dating back to the 1950s indicates that SC is feasible (e.g., see [4–6]). However, in the European Union (EU) and elsewhere, there seems to be a mindset that to develop a workable SCRJ propulsion system will take decades. At the same time, research and development in the United States, Russia, and China has produced research hypersonic craft powered by SCRJ, or combined cycles using SC, and flight testing is being planned [7]. This apparent contradiction is frustrating and stimulating at the same time.

What is a SCRJ-powered hypersonic vehicle? In essence, it is a thermal engine. Heat enters its box from outside (due to friction work and wave compression); from the inside (combustion heat), heat is rejected (radiatively or regeneratively to the fuel [8]), and work is done by thrust and drag to maintain steady-state operation, as in cruisers, or to increase the kinetic energy (KE) of the vehicle, as in accelerators. This picture of a hypersonic airbreathing vehicle is painted because it has strong implications on SC: large heat fluxes will enter and exit the combustor, affecting its velocity and temperature flowfield and ultimately its performance. This notwithstanding, SC is analyzed in this paper without including these effects, as they depend on specifics of the combustor design.

In a SCRJ the flowpath velocity changes little, whereas pressure may increase by one–two orders of magnitude [8]. The net thrust is the result of adding heat of reaction to the stream tube, but the ratio between combustion heat release and airstream kinetic energy, $\Delta H_{\text{reaction}}/\frac{1}{2}V_{\text{air}}^2$, is a small number (0.1 to 0.2) in hypersonic propulsion, so inlet, nozzle, and energy fluxes must be carefully designed to prevent negative cycle efficiency. The second principle of thermodynamics dictates that the maximum fraction of energy that may be transformed into useful work [9–11]: i.e., the net thrust times the flight speed. The net thrust is gross thrust T minus drag D, and both are very large. Thus, D must be controlled and reduced as much as possible. In particular, the friction work rate scales as ρV_{air}^3, where V_{air} is approximately constant but density grows by an order of magnitude or more due to inlet compression. Hence, *engine* friction drag is substantial and comparable with the *vehicle* total drag; hence, the combustor must be very short (of order 1 m). This conclusion seems obvious; however, there are some who believe that either combustor length should be $\mathcal{O}(10)$ m to compensate for the short residence time or that flame anchoring in a supersonic stream is next to impossible (witness the notorious simile of holding a candle in a storm). These beliefs, or mindsets, may produce proposals and programs to investigate the *feasibility* of SCRJ, but history shows that more often than not they derail good research.

Engineeringwise, the constraint on combustor length should suggest reassessing how fast mixing and kinetics should be *made* to ensure reasonable combustion efficiency. Said otherwise, since no first principle forbids SC, it is up to us to devise ways of enabling it.

In this context, it is known that in the Mach regime in which SC starts to become effective, the air stagnation temperature is greater than 1000 K, pressure may be of order 1 atm, spontaneous oxidation is fast, and flames may be stable even without a flameholder, depending on fuel and injection strategy. Typical kerosenes ignite in air at lower temperatures than hydrogen, but their kinetics are slower (however, actual experiments with ramp injectors [12] have shown that the *apparent* ignition delay and combustion time in SC of kerosene may be as low as 30 to 40 μs). Partly motivated by the specifications of the EU-funded Long-Term Advanced Propulsion Concepts and Technologies (LAPCAT) project [13], the fuel of choice in the present work is hydrogen, the application is a cruiser, and, although very interesting, SC of kerosene will not be discussed. Hydrogen injection into an airstream is characterized by the velocity, kinetic energy, and density ratios [14,15], all depending on hydrogen reservoir conditions and injection strategy once the flight Mach number is imposed. Pylons, struts, cavities, and flush holes create different recirculation zones and flowfields, impacting on flame anchoring and combustion efficiency. To zeroth order, the most important anchoring parameters are mixing time t_d (and mixedness), the kinetics time t_k, and the residence time t_r in the mixing zone. These are heuristic quantities, but still useful to estimate performance.

Kinetic time depends on mixedness, density, and temperature. Hydrogen should be injected at high speed but without quenching ignition kinetics, so there is a tradeoff between its internal and KE. In general, hydrogen stagnation enthalpy must be much higher than that typical of many (academic) experiments. In fact, in an actual SCRJ-powered vehicle, hydrogen works first as a coolant and then is injected as a *hot* gas, something experimenters are typically very reluctant to do. (This fact should be kept in mind when reading the conclusions of SC experiments.) One consequence is that there is a lower limit for the stagnation temperature of air: roughly speaking, that must be high enough for autoignition of H_2/air mixtures. At air $T > 1000$ K, kinetics are fast ($t_k \sim 0.1$ ms or less) and combustion is then mixing-controlled [16]; at lower air temperature (e.g., when transitioning from RJ to SCRJ mode), the opposite may be true (see [15]). Thus, the main concern is how to mix hydrogen to air in the turbulent, compressible, and reactive regimes, a process far less understood than chemical kinetics. Assuming that kinetics are fast, the ratio t_d/t_r should be small enough to minimize the length of combustor, its friction drag, and total vehicle size.

These remarks have implications in SC modeling. Assuming air static temperature less than 1000 K allows a preliminary zeroth-order analysis of the SCRJ combustor as a stirred reactor [17], with combustion occurring inside the fine turbulent structures, where fuel and oxidizer can mix at molecular scales. Swithenbank and Chigier [14] found the zeroth-order functional dependence of combustion efficiency η_c to be

$$\eta_c = 1/[1 + (t_d/t_r) + (t_k/t_r)\exp(1/\theta)]$$

where the function θ is of the Arrhenius form $E_A/(RT)$ and accounts for *ignition* kinetics [14,17]. The residence time t_r scales as the ratio of distance/streamwise velocity, x/U, both quantities defined *inside the mixing region*: i.e., where turbulent KE, generated mainly by the

interaction between airflow and fuel jet and transporting scalars, is *dissipated* by vortices. Note that this region is a fraction of the overall combustor (in cross injection of fuel, for instance, it is the recirculation and shear-layer region). In the incompressible regime, the so-called dissipation occurs via vortex stretching in the Kolmogorov inertial range. In supersonic mixing. it can still be assumed that the dissipation rate of KE is proportional to the mixing rate, but the real question concerns the dissipation mechanism(s) and the scaling of KE with eddy size (see Sec. II). Thus, t_d, the turbulent diffusion (or mixing) time scales as l_T, the average energy-containing eddy scale (for instance, the Taylor scale), divided by its fluctuation (or turnover) velocity u'. In a well-designed SCRJ combustor, it is the injection system that *must* generate turbulent KE, and l_T scales with its characteristic length L. If kinetics are fast ($t_k/t_r \ll 1$), efficiency depends only on mixing, and

$$t_d/t_r \sim (x/U)(u'/l_T)$$

where both x and l_T scale with L. The mixing-region size is expected to be larger than the injector size by a large factor (say, 50), yielding

$$t_d/t_r \sim 50(u'/U)$$

but note that this factor may depend on injection mode: for instance, dividing the mass flow rate of fuel among many injectors reduces this factor, and an optimum injector size may exist [8].

Thus, to zeroth order, the normalized mixing time depends on turbulence intensity only. Because inlet turbulence is generally small in supersonic flow, it is the fuel injection system that must produce it. Fuel injection must also account for the equivalence ratio desired (note that this may be less than 1) via penetration calculations (e.g., see [14,18]). For instance, for $u'/U = 5\%$, the mixing time will be two–three times the residence time in the region where turbulence is created by the injector(s), and η_c will be $1/1.4 = 0.7$.

Although this approach may seem overly simplified, it shifts SC from the realm of next-to-impossible to that of engineering: in particular, producing sufficiently fast and hard fuel jets.

There is, in fact, past evidence [19] that SC over a flat plate with 90 deg hydrogen injection through multiple holes can take place within $\mathcal{O}(1)$ ft, contradicting conventional wisdom saying that compressible mixing of two parallel streams needs a much longer distance than incompressible mixing [20]. This well-known conclusion was due to imposing a 2-D topology on the experiment [20]: an experiment carefully planned around good access to optical diagnostics. Much later, when the airflow was allowed to maintain its real life 3-D character, that conclusion was reversed [21,22]: supersonic mixing distance was shorter. All of these considerations indicate that, except for some work [23–42], the detailed physics of turbulent, compressible, and reactive flows is still poorly understood and has not received all the attention it deserves. This is so much so that turbulence and flame models in 3-D Favre-averaged Navier–Stokes (FANS) simulations or large-eddy simulation (LES) of subsonic flows are almost invariably also used at Mach > 1; when they are not, turbulent diffusion is purposely made slower, to account for the results in [20].

In summary, the purpose of this paper is to contribute toward improving the understanding of turbulent reactive flows, focusing on turbulence and chemistry taking place in a supersonic airstream representative of SCRJ applications, with the ultimate goal of providing more physically realistic closures for FANS and LES.

II. Mach Number Effects on Turbulence

This section includes a theoretical analysis of the effects of compressibility (Mach number) on turbulence and combustion. Prior work [14,23–37,43–52] has already indicated that supersonic internal flows are characterized mainly by streamwise vorticity and thus by maximum helicity ($H = \bar{\omega} \cdot \bar{u}$). As shown by Nishioka et al. [31] and Swithenbank et al. [8,14,17], streamwise vorticity enhances supersonic mixing down to the molecular scales and leads to efficient combustion. Further, due to high helicity, turbulent KE decay is significantly affected by baroclinic and dilatational effects and is faster with respect to the classic Kolmogorov scaling for constant-density flows [31,32,41,42,53–55]. The Kolmogorov spectrum shows two ranges: the inertial, where energy is transferred from smaller to higher wave numbers (from larger to smaller vortices) without dissipation, and the dissipative range, where viscous effects are important. It has also been found that mixing can be improved by forcing transversal pressure gradients, e.g., by means of particular flowpath configurations (such as favoring shocklet formation) and devices (injectors) [31,36,43–47]. Furthermore, it has been shown that supersonic combustion takes place at approximately *locally* constant volume [23,24,32,56,57] and that collisional frequency increases due to *local* nonequilibrium (negative) dilatation, resulting in faster kinetics and thus higher flame speed and thinner flames. Note also that typical inlet turbulence *intensity* is lower than in subsonic flows and of the order of a few percentage points [51,58]. The reason is that at increasing Mach numbers, the KE of the bulk flow increases with respect to thermal and so does the pressure gradient necessary to change momenta and drive fluctuations; at the same time, an eddy's turnover *velocity* can be much larger than in subsonic flows. The scale of dissipative eddies is also shown to be larger [31], implying combustion regime(s) possibly different from those typical of subsonic flows at the same Reynolds and Damköhler numbers.

All of this supports the conclusion that understanding of the flame regime in supersonic flows is crucial for the choice of the chemistry/turbulence coupling (that is, of the closure model for energy and species equations) and, in the end, for realistic SC simulations. Such understanding is easier when analyzing the equation for vorticity ω rather than the momentum (Navier–Stokes) equation.

By using as reference quantities at the combustor inlet [that is, u_0 (x velocity component), L_0 (eddy macroscale), $t_0 = L_0/a_0$ (where a_0 is the speed of sound), ρ_0, and $p_0 = \frac{1}{2}\rho_0 u_0^2$], the nondimensional equation for ω is

$$\frac{1}{Ma}\frac{\partial \bar{\omega}}{\partial t} + (\bar{u}\cdot\bar{\nabla})\bar{\omega} = \bar{\omega}\cdot\overline{\overline{\nabla u}} - \bar{\omega}(\bar{\nabla}\cdot\bar{u}) + \frac{\overline{\nabla\rho}\times\overline{\nabla p}}{\rho^2} + \frac{1}{Re}\nu\overline{\overline{\nabla^2\omega}} + \frac{1}{Re}\left(-\frac{1}{\rho^2}\overline{\nabla\rho}\times(\bar{\nabla}\cdot\bar{\bar{\sigma}}) + \frac{1}{\rho}(\overline{\nabla\mu}\times(\overline{\nabla^2 u} + \bar{\nabla}(\bar{\nabla}\cdot\bar{u})) + 2\bar{\nabla}\times(\bar{\bar{E}}\,\overline{\nabla\mu}))\right) \quad (1)$$

with its symbolic budget

$$\frac{1}{Ma}I + \text{conv} = \text{VS} - \text{CP} + B + \frac{1}{Re}\text{diff} + \frac{1}{Re}(-\text{CV} + \text{VV} + \text{DV}) \quad (2)$$

where I, conv, VS, CP, and B are, respectively, the inertial, convective, vortex stretching, dilatational, and baroclinic terms; diff, CV, VV, and DV are the diffusive terms due, respectively, to viscous gradients, the coupling between density gradients and viscous stresses, the coupling between viscous stresses and velocity gradients, and the coupling between strain rate and viscous gradients.

Equation (2) shows that in supersonic flows the dilatational term is of the same order of magnitude of the vortex stretching $(\bar{u}\cdot\bar{\nabla})\bar{\omega}$; thus, unlike subsonic flows, vorticity transport is *not* exclusively driven by vortex stretching, but also by compressibility and baroclinic effects. Further, since the inertial term is proportional to $1/Ma$, when increasing the Mach number, the so-called time-dependent fluctuations are less and less important and the flow tends toward steadiness.

The fact that internal flows of interest to SC are characterized by high Mach number mainly in the streamwise direction suggests the existence of two velocity scales: that of the supersonic streamwise u component and that of the transversal components v and w, where $u > a \gg v \approx w$ (flow anisotropy). If k_s is the ratio between the

transversal Mach ($Ma_{\text{sub}} = v/a$) and the streamwise Mach number ($Ma_{\text{sup}} = u/a$), that is,

$$k_s = \frac{Ma_{\text{sub}}}{Ma_{\text{sup}}} = \frac{v}{u}$$

then supersonic internal flows are characterized by $k_s \ll 1$. An interesting consequence can be gathered from the nondimensional continuity equation using the same reference quantities as before and $h_0 = \frac{1}{2}u_0^2$.

In Cartesian coordinates,

$$\frac{\rho_0}{t_0}\frac{\partial \rho}{\partial t} + \frac{\rho_0}{L_0}u_0\frac{\partial \rho}{\partial x}u + \frac{\rho_0}{L_0}v_0\left(\frac{\partial \rho}{\partial y}v + \frac{\partial \rho}{\partial z}w\right) + \frac{\rho_0}{L_0}u_0\rho\frac{\partial u}{\partial x} + \frac{\rho_0}{L_0}v_0\rho\left(\frac{\partial v}{\partial y} + \frac{\partial w}{\partial z}\right) = 0 \tag{3}$$

By introducing k_s, the continuity equation (3) becomes

$$\frac{1}{Ma_{\text{sup}}}\frac{\partial \rho}{\partial t} + \frac{\partial \rho}{\partial x}u + k_s\left(\frac{\partial \rho}{\partial y}v + \frac{\partial \rho}{\partial z}w\right) + \rho\frac{\partial u}{\partial x} + k_s\rho\left(\frac{\partial v}{\partial y} + \frac{\partial w}{\partial z}\right) = 0 \tag{4}$$

Since $k_s \ll 1$ and $Ma_{\text{sup}} > 1$, Eq. (4) can be rewritten as

$$\frac{\partial \rho}{\partial x}u + \rho\frac{\partial u}{\partial x} + \frac{1}{Ma_{\text{sup}}}\frac{\partial \rho}{\partial t} + k_s\left[\frac{\partial \rho}{\partial y}v + \frac{\partial \rho}{\partial z}w + \rho\left(\frac{\partial v}{\partial y} + \frac{\partial w}{\partial z}\right)\right] = 0 \tag{5}$$

Thus, the change of u with x is mainly balanced by a density change, not by local transverse velocity gradients. Neglecting viscous effects for the time being, the simplified nondimensional momenta equations are

$$\begin{cases} u\frac{\partial u}{\partial x} + k_s\left(\frac{\partial u}{\partial t} + v\frac{\partial u}{\partial y} + w\frac{\partial u}{\partial z}\right) = -\frac{1}{\rho}\frac{\partial p}{\partial x} \\ u\frac{\partial v}{\partial x} + k_s\left(\frac{\partial v}{\partial t} + v\frac{\partial v}{\partial y} + w\frac{\partial v}{\partial z}\right) = -\frac{1}{k_s}\frac{1}{\rho}\frac{\partial p}{\partial y} \\ u\frac{\partial w}{\partial x} + k_s\left(\frac{\partial w}{\partial t} + v\frac{\partial w}{\partial y} + w\frac{\partial w}{\partial z}\right) = -\frac{1}{k_s}\frac{1}{\rho}\frac{\partial p}{\partial z} \end{cases} \tag{6}$$

indicating that in ducted supersonic flows, even moderate gradients of pressure along y and z can generate significant v and w gradients, i.e., $\partial v/\partial x$ and $\partial w/\partial x$, in the streamwise direction. The presence of these $\partial v/\partial x$ and $\partial w/\partial x$ produces vorticity in the y and z directions, favoring mixing and (if temperature is appropriate) quick ignition and combustion. In fact, experimental results in [8,14,59] show that flame anchoring is favored by raising the fuel jet/air stagnation pressure ratio. The airstream per se does not carry significant turbulent KE, and to produce vorticity, KE must be created in some way: for instance, injecting fuel with the highest momentum that equivalence ratio and geometry constraints will allow and the appropriate jet-to-stream-density ratio [14,17,59].

Pressure gradients and vorticity may also be produced by combustion itself or by appropriately shaping combustor geometry and injectors (e.g., using ramp injectors [31]). Strong pressure gradients are also observed close to shocks, and in fact, they are known empirically to increase mixing and combustion, sometimes at the price of total pressure losses.

To support what was said about the influence of helicity, neglect viscous terms in the nondimensional x-vorticity equation and obtain

$$u\frac{\partial \omega_x}{\partial x} = \omega_y\frac{\partial v}{\partial x} + \omega_z\frac{\partial w}{\partial x} + \frac{1}{k_s}\frac{1}{\rho^2}\left(\frac{\partial \rho}{\partial y}\frac{\partial p}{\partial z} - \frac{\partial \rho}{\partial z}\frac{\partial p}{\partial y}\right) \tag{7}$$

Since $1/k_s \gg 1$, Eq. (7) shows that pressure and density changes along y and z influence the vorticity transport along x. The helicity $H = \bar{\omega}\cdot\bar{u}$ gives a reasonable idea of the *rotational acceleration* of the flow. When vorticity and velocity are aligned, helicity is maximum and the term $\bar{\nabla}\times(\bar{\omega}\times\bar{u})$, which includes vortex stretching, reaches a minimum. Thus, where helicity peaks, the vortex stretching term, responsible *in subsonic flows* for the turbulent KE cascade, becomes very small, and mixing is no longer driven or controlled by vortex stretching. This conclusion may also be derived from the inviscid nondimensional helicity equation,

$$H = \omega_x u + \frac{\partial u}{\partial z}v - \frac{\partial u}{\partial y}w + k_s\left(\frac{\partial v}{\partial x}w - \frac{\partial w}{\partial x}v\right) \tag{8}$$

showing that in supersonic ducted streams, where $k_s \ll 1$ (negligible $\partial u/\partial z$, $\partial u/\partial y$, v, and w), helicity may be approximated by $H \cong \omega_x u$: vorticity is mainly streamwise and helicity is large. Thus, in supersonic flows, vortex stretching is smaller than in subsonic flows, and where dilatational and baroclinic effects are negligible (e.g., far from shocks or flames), its contribution to KE transfer in the inertial range is less effective and characterized by fewer scales. If baroclinic and dilatation effects were missing, the slope of the turbulent KE-vs-wave-number curve would be steeper than that ($-5/3$) of the well-known Kolmogorov theory in incompressible flows. At the same time, in a flow dominated by streamwise vorticity, large-scale mixing may be much more efficient than when vorticity has no preferential direction. Thus, even though the effect of vortex stretching is less important than in the incompressible regime, the efficient mixing observed in some supersonic flow experiments cited must be driven by baroclinic and dilatational [31] effects. When combustor geometry and boundary conditions allow it, the supersonic flow may be described as being composed of helicoidal structures, and mixing may still be efficient and combustion distance may be short [11,19,31,35,48,49]. This conclusion is valid for fully 3-D flows: the experimental results of [20], in which streamwise turbulence was deliberately suppressed by the 2-D geometry, showed that the shear-layer growth rate reduces substantially with increasing compressibility, reaching about one-fifth of the incompressible value at high convective Mach numbers. In later papers, Papamoschou [21] and Papamoschou and Bunyajitradulya [22] showed that for convective Mach numbers greater than 0.5, the fully 3-D shear-layer growth rate was 25% *higher* than in the incompressible case and had *improved* mixing. That is also the conclusion in [14,31–40,43–52], in which streamwise vorticity was found to enhance mixing at the molecular level, leading to short flames and efficient combustion.

The few recent direct numerical simulations (DNS) in compressible flows tend to confirm these theoretical results. References [53,54,60,61] noted that in (nonreacting) supersonic flows, the baroclinic term plays an important role in vortex production near shocks and that compressibility amplifies vorticity, whereas far from shocks, vortex stretching again becomes the main mixing driver. Other DNS of supersonic flows confirm turbulence are mainly streamwise, with velocity and vorticity generally angled either at 0 or 180° [61].

As a further check, the functional dependence of the energy spectrum in supersonic flows has been derived here by means of the Buckingham–Riabucinski π theorem. In supersonic flows, the turbulent kinetic energy density per unit wave number, E, depends on the wave number k, the rate of energy dissipation per unit volume ε, and the flow density, now an independent variable.

The dimensions of these variables are

$$k = \frac{1}{\text{length}} \tag{9}$$

$$\varepsilon = \text{mass}\frac{\text{length}^2}{\text{time}^3} \tag{10}$$

$$\rho = \frac{\text{mass}}{\text{length}^3} \tag{11}$$

$$E = \text{mass}\frac{\text{length}^3}{\text{time}^2} \tag{12}$$

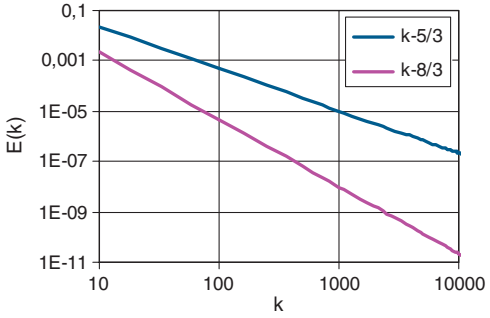

Fig. 1 Energy density vs wave number.

Assuming that E depends on k, ρ, and ε, the energy density per unit wave number is $E(k, \rho, \epsilon)$ and must be expressed as $Ck^{\alpha}\rho^{\beta}\epsilon^{\gamma}$, where C is a constant. The exponents α, β, and γ are found to be $-8/3$, $2/3$, and $1/3$, respectively.

Thus, with the previous assumptions,

$$E(k, \rho, \varepsilon) = Ck^{-8/3}\rho^{1/3}\varepsilon^{2/3}$$

whereas in subsonic flows, $E(k, \varepsilon) = Ck^{-5/3}\varepsilon^{2/3}$ (see Fig. 1).

If compressibility affects the energy density, the scaling law for the transfer of kinetic energy from larger to smaller scales must be different. In particular, the steeper slope means that energy starts to be dissipated at lower wave numbers: in supersonic flows, dissipative eddies are larger than in subsonic flows. This is experimentally confirmed in [31,41,42,55]. This is an important conclusion, since in SCRJ, mixing and burning must be very fast; furthermore, in SC flames the smallest eddies may actually be larger than the flame thickness and, if so, they can only wrinkle the flame without thickening it. These findings are further supported in [33] and have led to more efficient fuel injectors [31].

III. Effect of Compressibility on Reaction Rates

A second aspect of compressibility is the effect of dilatation on chemical kinetics. At the simplest modeling level (Arrhenius), the reaction rate $\dot{\omega}$ is defined in terms of effective collisional frequency per unit volume, z_V [62]. For instance, in a bimolecular reaction between reactants X and Y,

$$\dot{\omega} = \frac{1}{N_A} z_V e^{-\frac{E_A}{\Re T}} = \frac{\sqrt{\pi}}{N_A}\sigma^2\sqrt{8\frac{\Re T}{\mu M}}e^{-\frac{E_A}{\Re T}}[X][Y] \tag{13}$$

where square brackets indicate molar concentrations.

From the classical expression for the reaction rate,

$$\dot{\omega} = AT^{\frac{1}{2}}e^{-\frac{E_A}{\Re T}}[X][Y] \tag{14}$$

the Arrhenius preexponential A is therefore 63:

$$A = \frac{2}{N_A}\sqrt{2\pi\frac{\Re}{\mu M}}\sigma^2 \tag{15}$$

Strictly speaking, Eq. (13), derived from gas kinetic theory, is valid only in the case of thermodynamic equilibrium (Maxwell–Boltzmann distribution). In supersonic flows, where acoustics is slower than convection, thermodynamic equilibrium becomes questionable, just as inside a shock wave it is not possible to define an equilibrium thermodynamic temperature [63]. At the molecular scale where reactions occur, compressibility implies local mean free paths that are shorter (collisional frequency that are higher) than predicted by Eq. (13). Some of the effects of compressibility on chemistry have been studied [64–67], but this nonequilibrium effect needs further exploring. In fact, the z_V predicted by gas kinetics corresponds to the zeroth-order solution of the Boltzmann equation using the Chapman–Enskog expansion, the zeroth order being associated with the assumption of zero bulk velocity. The first-order Chapman–Enskog solution accounts for finite flow velocity and includes the effect of compressibility. A few first-order models have been developed [66,67] to understand how this effect influences collisional frequency; however, some yield a correction to the Arrhenius exponential term that does not satisfy the second law of thermodynamics.

To rigorously evaluate this effect on reaction rate in high-speed flows, z_V should be calculated from the Boltzmann equation. This would be a forbidding task. The much cruder but practical alternative [23] is to analyze the effect of a (small) displacement from local equilibrium. Expanding the function $z_V\ (t, \rho, T, M)$ of Eq. (13) around the equilibrium instant t_0 yields

$$z_V = \frac{z}{V}(t, \rho, T, M) = \frac{z}{V}\bigg|_{t=t_0} + \frac{1}{1!}\frac{Dz}{Dt}\bigg|_{t=t_0}(t - t_0) + \frac{1}{2!}\frac{D^2z}{Dt^2}\bigg|_{t=t_0} \times (t - t_0)^2 + \frac{1}{3!}\frac{D^3z}{Dt^3}\bigg|_{t=t_0}(t - t_0)^3 + \ldots \tag{16}$$

and to first order,

$$\frac{z}{V}(t, \rho, T, M) = \frac{z}{V}\bigg|_{t=t_0} + \frac{Dz}{Dt}\bigg|_{t=t_0}(t - t_0) + \mathcal{O}(2) \tag{17}$$

By differentiating the collisional frequency with respect to time,

$$\frac{D(\frac{z}{V})}{Dt} = 2\sqrt{\pi\Re}(nN_A\sigma)^2\frac{D(\rho^2\sqrt{\frac{T}{M}})}{Dt} = 2\sqrt{\frac{\pi\Re}{M}}(N_A\sigma)^2\left(n^2\sqrt{T}\frac{D(\rho^2)}{Dt} + n^2\rho^2\frac{D(\sqrt{T})}{Dt} + \rho^2\sqrt{T}\frac{D(n^2)}{Dt}\right) \tag{18}$$

the following expression is obtained:

$$\frac{D(\frac{z}{V})}{Dt} = 2\sqrt{\frac{\pi\Re}{M}}(nN_A\sigma)^2\rho^2\sqrt{T}\left(2\frac{D\rho}{Dt} + \frac{1}{2}\frac{DT}{Dt} + 2\frac{Dn}{Dt}\right) \tag{19}$$

Consequently,

$$\frac{z}{V}(t, \rho, T, M) = \frac{z_0}{V}\left[1 + \left(\frac{2}{\rho}\frac{D\rho}{Dt} + \frac{1}{2T}\frac{DT}{Dt} + \frac{2}{n}\frac{Dn}{Dt}\right)\bigg|_{t=t_0}(t - t_0)\right] + \mathcal{O}(2) \tag{20}$$

Equation (20) tells that collision frequency changes due to changes of density, temperature, and number of moles. Dilatation effects are due to $D\rho/Dt$. The second term, DT/Dt, is negligible if the time for the temperature to increase (due to combustion) is longer than the chemical time: in this case, the temperature rise does not affect collisional frequency.

Also assuming that the molar volume change is small for hydrogen combustion with air, DT/Dt and Dn/Dt may be neglected, and Eq. (20) simplifies to

$$\frac{z}{V}(t, \rho, T, M) = \frac{z_0}{V}\left[1 + \left(\frac{2}{\rho}\frac{D\rho}{Dt}\right)\bigg|_{t=t_0}(t - t_0)\right] \tag{21}$$

By combining Eq. (21) with the continuity equation

$$\frac{D\rho}{Dt} + \rho(\bar{\nabla}\cdot\bar{u}) = 0$$

Eq. (21) becomes

$$\frac{z}{V}(t, \rho, T, M) = \frac{z_0}{V}[1 - 2\bar{\nabla}\cdot\bar{u}|_{t=t_0}(t - t_0)] \tag{22}$$

showing that the influence of compressibility on collision frequency is negligible in subsonic flows ($\nabla\cdot\mathbf{u} \cong 0$) and may become important in supersonic flows. The consequences on reaction rate requires some more manipulation. By writing $\rho = \rho(p, T, R)$,

$$\frac{D\rho(p,T,R)}{Dt} = \frac{\partial\rho}{\partial p}\frac{Dp}{Dt} + \frac{\partial\rho}{\partial T}\frac{DT}{Dt} + \frac{\partial\rho}{\partial R}\frac{DR}{Dt} \tag{23}$$

and if, for the time being, we deal here *only with the acoustics contribution* (i.e., that due to pressure),

$$\frac{D\rho(p,T,R)}{Dt} = \frac{\partial\rho}{\partial p}\frac{Dp}{Dt} = \frac{1}{a^2}\frac{Dp}{Dt} \tag{24}$$

where $a^2 = \partial p/\partial\rho$.

By combining Eq. (24) with the continuity equation

$$\frac{\partial u_i}{\partial x_i} = -\frac{1}{\rho a^2}\left(\frac{\partial p}{\partial t} + u_i\frac{\partial p}{\partial x_i}\right) \tag{25}$$

and using dynamic pressure as the reference pressure, Eq. (25) becomes

$$\frac{\partial u_i^*}{\partial x_i^*} = -Ma_s^2\frac{1}{\rho^* a^{*2}}\left(\frac{\partial p^*}{\partial t^*} + u_i^*\frac{\partial p^*}{\partial x_i^*}\right) \tag{26}$$

where the superscript * indicates nondimensional quantities and Ma_s is the *subgrid-scale* (SGS) Mach number associated with the SGS velocity fluctuation. This SGS fluctuation and its Mach number are extracted from the SGS model for the turbulent KE and the turbulent viscosity closure (see [24]). Equation (26) shows that the divergence of velocity scales with Ma_s^2, so that

$$z_V(t,\rho,T,M) \sim z_{0_V}\left[1 + 2Ma_s^2\frac{\Delta p^*}{\rho^* a^{*2}}\right] \tag{27}$$

The sign will be + where $\bar{\nabla}\cdot\bar{u} < 0$ and will be − where $\bar{\nabla}\cdot\bar{u} > 0$. Thus, in compressible flows the collisional frequency depends on the local Mach number and so does, accordingly, the reaction rate:

$$\omega(t,\rho,T,M) = \omega_0\left[1 + 2Ma_s^2\frac{\Delta p^*}{\rho^* a^{*2}}\right] \tag{28}$$

The SGS Mach number depends on the turbulence intensity, of order 1 to 10%. For instance, assuming an airstream $M = 2.5$ and turbulence intensity 1 to 10%, the term $(1 + 2M_s^2)$ ranges from about 1.00125 to 1.125, i.e., compressibility enhance the reaction rate by about 0.125 to 12%. In the simulations reported in Sec. VI, whenever combustion was intense, the turbulence intensity was of order 10%.

Equation (28) predicts rates growing when $\bar{\nabla}\cdot\bar{u} < 0$, i.e., when locally the flow compresses; where the flow expands sufficiently rapidly, the collisional frequency slows down and so does the reaction rate. In summary, crude as it is, this model predicts that there is an effect of *local (SGS) Mach number* on reaction rates that is negative where flow expands and positive where flow compresses. Note, however, that wherever the flow expands, the temperature decreases and kinetics slows down anyway: the effect of the Mach number on kinetics when dilatation is positive is not as significant as when flow compresses. Remember also that only one of the three terms in Eq. (23) was modeled. The others will also be modeled in the future.

Because of the crude assumptions employed, this new model for $\dot{\omega}$ should still be further tested; yet, it might explain the prompt flame anchoring shown by old experimental results and still be hard to simulate. For instance, supersonic combustion tests at NASA Dryden Research Center in 1961–1962 [19] with nominal airstream Mach = 3.9, $T_0 = 2390$ K, and $P_0 = 0.29$ atm were carried on with hydrogen injected in crossflow through a row of eight holes on a flat plate.

Shadowgraphs and infrared (IR) fast-camera pictures shown in Fig. 2 indicate that ignition was fast and the flame was well-anchored. The picture on the right was taken with a IR filter and shows water [19]. If, as it appears, at $M > 1$ compressibility does indeed affect reaction rates, *this effect must be taken into account in modeling chemical kinetics*.

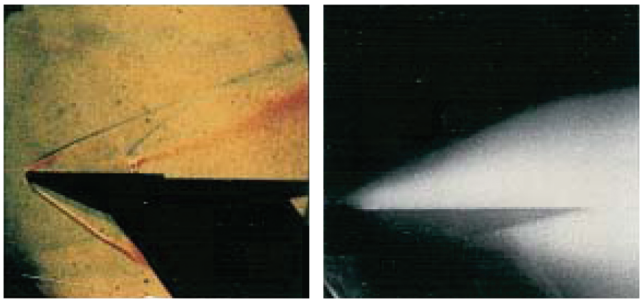

Fig. 2 Supersonic combustion flame anchoring on a flat plate.

IV. Effect of Mach Number on Flame Regime

The understanding of regime is preliminary to choosing a model describing turbulence/combustion coupling and, in particular, to model the filtered reaction-rate equations closing the filtered species equations. In fact, with typical LES filter width, chemical reactions occur within the subgrid scale and must be modeled. In SC, flames are nonpremixed and two limiting cases exist: slow and fast chemistry. In the slow-chemistry limit, turbulent mixing may occur before reacting, and at small scales, this situation approaches a well-stirred reactor. This case is typical of relatively low flight Mach numbers (e.g., 6 to 8). At Mach > 8 the opposite is typical: kinetics are faster than mixing.

In modeling *incompressible* turbulent premixed flames, five parameters are of importance and characterize the flame regime: l_k/δ_l, L_0/δ_l, Re, Da, and v'/S_l, where L_0 is the integral turbulence scale, l_k is the dissipative scale, δ_l is the flame thickness, v' is the eddy turnover velocity, and S_l is the laminar flame speed. These parameters define three different regimes: distributed reactions, wrinkled laminar flames, and corrugated flames.

Defining a reference kinematic viscosity n_{ref} as $\nu_{\text{ref}} = S_l\delta_l$, the turbulent Reynolds, Damköhler, and Karlovitz numbers are

$$Re = \frac{v'L_0}{S_l\delta_l} \qquad Da = \frac{t_{\text{conv}}}{t_{\text{chem}}} = \frac{S_lL_0}{v'\delta_l} \qquad Ka = \frac{1}{Da_k} = \frac{t_{\text{chem}}}{t_k} = \frac{v_\eta^2}{S_l^2} = \frac{\delta_l^2}{\eta^2} \tag{29}$$

The Karlovitz number is an inverse Damköhler number at which the dissipative time scale replaces the integral time scale. From Eq. (29), it follows that

$$\frac{v'}{S_l} = Re\left(\frac{L_0}{\delta_l}\right)^{-1} = \frac{1}{Da}\frac{L_0}{\delta_l} = Ka^{2/3}\left(\frac{L_0}{\delta_l}\right)^{\frac{1}{3}} \tag{30}$$

Plotting the logarithm of v'/S_l vs the logarithm of L_0/δ_l yields the Klimov–Williams diagram for premixed combustion (see Fig. 3). The lines $Re = 1$, $Da = 1$, and $Ka = 1$ are boundaries between the different regimes of premixed turbulent combustion. A similar diagram (Borghi's diagram) is obtained by plotting $\log(Da)$ vs $\log(Re)$ (see Fig. 4).

In Fig. 3 the line $Re = 1$ separates laminar (upper) from turbulent (lower) regimes. $Da \gg 1$ means that kinetics are very fast compared with transport, and the assumption of fast chemistry (and that of a global mechanism) may then be justified.

Depending on the turbulence intensity, the flame is wrinkled or corrugated. In particular, if $Ka < 1$ and $\delta_l \ll l_k$, the smallest eddies are larger than flame thickness and the flame is only corrugated (not much stretched) by eddies. The line $v'/S_l = 1$ separates wrinkled from corrugated flamelets. Where $v' < S_l$, the turnover velocity of the large eddies, v', is slower than that of the flame front: large eddies cannot convolute the flame front enough to form multiple reaction sheets.

Within the regime of corrugated flamelets, the velocity of large eddies is larger than the burning velocity S_l, and these eddies will move the flame front about, causing substantial convolution. The smallest eddies, with turnover velocity less than S_l, will not wrinkle the flame front. Vice versa, if $Ka > 1$ and $l_k < \delta_l < L_0$, the flame is

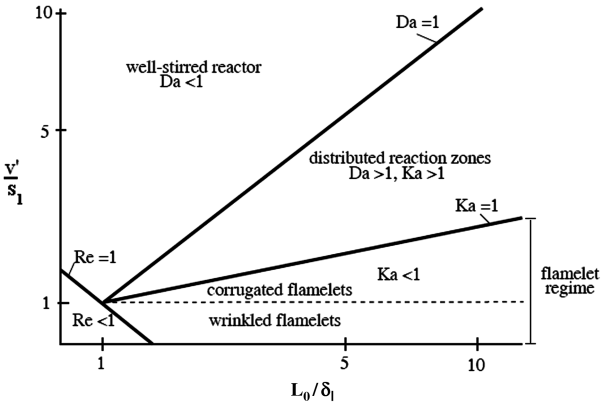

Fig. 3 Klimov–Williams diagram in the subsonic regime.

distributed: the smallest eddies enter into the flame, thickening its structure. Finally, in the well-stirred reactor regime characterized by $Ka > 1$ and $Da < 1$, chemistry is so slow compared with turbulent transport that the regime is that of a well-stirred reactor.

In *supersonic* flows, compressibility affects flame speed by (at least) increasing the reaction rate by a factor $1 + 2Ma_s^2$; accordingly, flame speed is increased by the factor $\sqrt{1 + 2Ma_s^2}$, and the lines in Fig. 4 translate upwards. The blue bold lines in this figure are the boundaries for $M = 0.3$, the fuchsia bold lines are for $Ma = 1$, and the red bold lines are for Mach $= 3$. This compressibility effect alters the boundaries reaction regimes with respect to incompressible flow, as shown in Fig. 4.

At $Ma < 1$, for Zel'dovich number

$$Z = \frac{\Delta T_c}{T_0}\frac{T_a}{T_0} \gg 1$$

and low turbulence, a reaction-sheet regime is predicted by Bray et al. [68] both for subsonic and supersonic combustion. However, what was said about reaction rate and spectrum may significantly affect predictions and conclusions in [68].

For example, at flight Mach ~7–9 (combustor $Ma \sim 1$–3), inlet combustor temperatures are greater than 1000 K and hydrogen/air chemistry is fast; using fast or global kinetics are acceptable, although not truly realistic. LES simulations in [26] and LES results reported in Sec. VI predict turbulence intensity ~0.5 to 10%, depending on injection strategy and combustor geometry. With these numbers, the turbulent large-scale Reynolds numbers estimated from the simulations are in the range of

$$Re_t = \rho U_0 L_0/\mu = 2000\text{–}100,000$$

and the turbulent large-scale Da_t, defined as

$$Da_t = \frac{L_0/U_0}{(\dot{\omega}/\rho)^{-1}}$$

is in the range of 9–2000. The flame speed $S_l = \sqrt{D\dot{\omega}_{Ma>1}}$ has been calculated by imposing the Arrhenius reaction rate defined as

$$\dot{\omega}_{Ma>1} \propto \dot{\omega}_{Ma<1}(1 + 2Ma_s^2)$$

and the reaction rate at $Ma > 1$ is that calculated from LES simulations (see Fig. 5). The flame thickness is then derived as the ratio between flame speed and chemical time, and these are also calculated from the reaction rate.

The ranges of values for Reynolds and Damköhler numbers and for the l_k/δ_l, L_0/δ_l, and v'/S_l just obtained define where supersonic combustion can occur and thus define possible flame regimes. These are shown in Fig. 6, indicating that in SC, either the flamelet in eddies regime or the reaction-sheet regime are possible, depending on the local Mach number. Larger Mach numbers raise the likelihood of flamelet in eddies. If so, the model for the turbulence-chemistry coupling could be based on an eddy dissipation concept, where the reaction rate is controlled by both mixing and chemistry [69].

In the experience of the authors, all the above theoretical considerations are hardly capable of removing the skepticism mentioned in

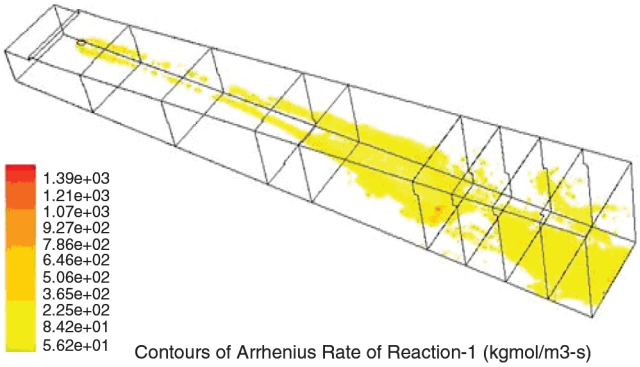

Fig. 5 LES-predicted contour of the Arrhenius reaction rate.

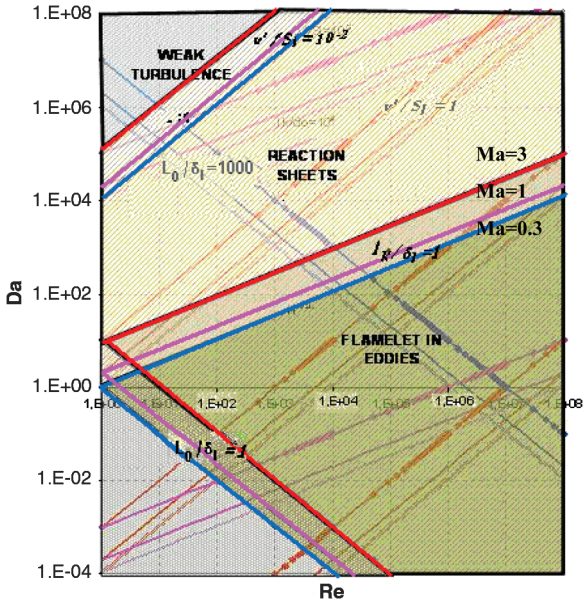

Fig. 4 Reaction regimes boundaries as a function of Mach numbers.

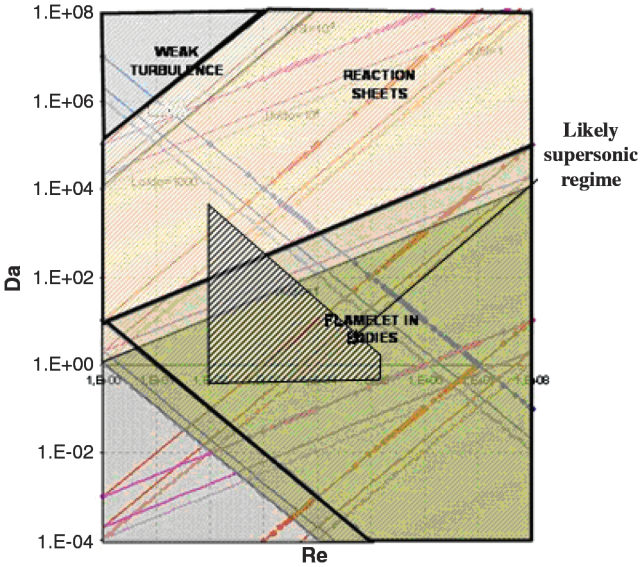

Fig. 6 Most likely SC regimes.

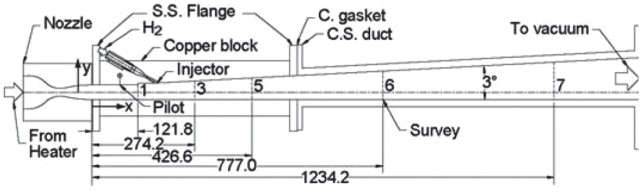

a)

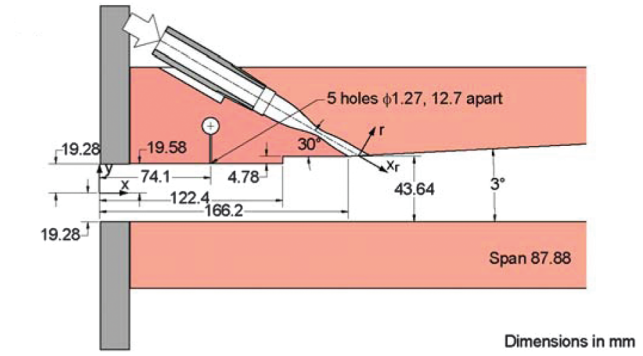

b)

Fig. 7 LaRC SCHOLAR facility: a) nozzle and combustion chamber and b) details of the H_2 injector.

Sec. I and that typically asks for proof based on CFD simulations. Most of the time, approximations made in modeling, numerical consistency and accuracy, and grid size do impact such proofs. Nevertheless, this being the state of affairs, the turbulence and chemistry closures developed by the authors since 2003 and described in this paper have been embodied in a set of subroutines under the name of Ingenito supersonic combustion modeling (ISCM) model [23–30]. LES of a open-literature test case based on an experimental campaign at the NASA Langley Research Center (LaRC) in the late 1990s through early 2000s were performed to check the ISCM model predictive capability. The experimental data used in the LES reported below were consistent with the flamelets-in-eddies regime. As a consequence, the eddy dissipation concept was implemented to deal with the turbulence-chemistry coupling.

V. LaRC Test Case: Geometry and Experimental Results

The test case and results have been reported before [23–30] and will be only summarized. A direct-connect combustor was used to measure temperatures and pressures in SC of H_2 and air experiments during the SCHOLAR LaRC program [49] (see Figs. 7 and 8). Combustion-heated vitiated air is introduced at Mach 2, 1184 K, and 100,405 Pa.

Simulations with the ISCM model were restricted to 800 mm of the whole length (1234 mm) of the SCHOLAR combustor: the inlet plane $X = 0$ in the simulations corresponds to the plane $X = 77$ mm of the experiments. In Fig. 8, a 3-D view of the experimental average temperature field is shown. Experimental results indicate the flame anchors between cross sections 5 and 6. As the latter section is 77 cm from the combustor inlet plane and about 60 cm from the H_2 injector, mixing times can be reasonably well estimated to be $\sim 5 \times 10^{-4}$ s, in good agreement with the arguments and scaling discussed in Sec. I. Maximum (averaged) temperatures are ~2200 to 2300 K. Unfortunately, no velocity or concentrations were measured at the exit, preventing assessment of η_c. However, reproducing the experimental flame attachment (without any flameholder) is a good test of the physics embodied by the ISCM model.

A. Numerical Scheme

The double-precision 3-D LES were performed with FLUENT 6.3. The numerical scheme is a coupled explicit third-order-in-space MUSCL and is second-order implicit in time.

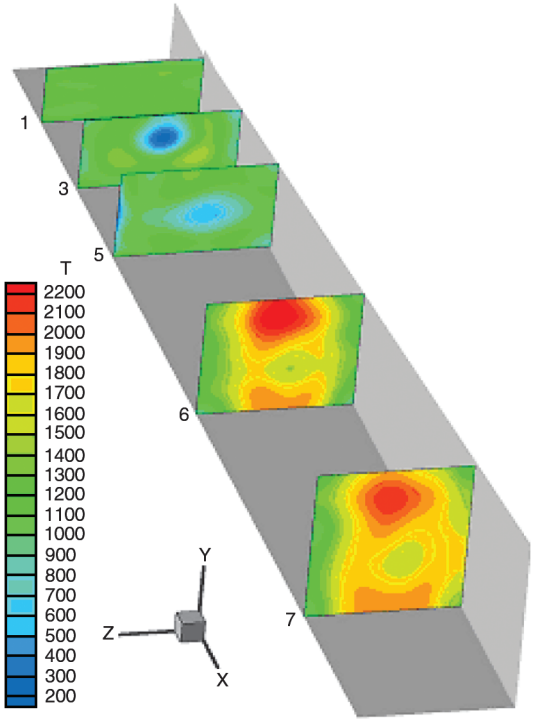

Fig. 8 Three-dimensional view of the measured (averaged) temperatures.

B. Computational Domain

The domain in Fig. 9 was discretized with a nonuniform 700 streamwise by 46 cross stream by 60 spanwise grid, finer near the step and fuel injector. The number of hexahedral cells was 1,563,994, for a total of 1,626,578 nodes. Wall $Y+$ of orders 4–8 were obtained near the step and H_2 injector orifice (see Fig. 9), where the NASA experiment predicts shock formation.

C. Inlet Boundary Conditions

Calculations begin at the $X = 0$ station of the SCHOLAR combustor, where vitiated air from the heater enters the duct at $Ma = 2.0$ (1395.7 m/s), 1204 K, and 101,325 Pa. Mole fractions of vitiated air species are in Table 1. The H_2 is injected at Mach 2.5, 1343 K, and 202,650 Pa. The nominal equivalence ratio is close to 1.

The combustor walls were nonadiabatic: the wall heat flux imposed (from the experiment) varies linearly from 0.7 to 1.8 MW/m^2 along the X direction. The total heat lost through the walls corresponds to about 10% of the combustion heat release. No-slip conditions were specified along the channel walls.

D. Turbulence and Chemistry Models

The turbulent viscosity closure of the ISCM model has been already reported [23]. A novel SGS model for the turbulent Schmidt number has been included [29] but is not reported here. Based on the conclusions in Sec. IV, air/H_2 kinetics have been modeled by the global scheme [70]:

Table 1 Vitiated air mole fractions at the inlet

Species	Value
H_2	OH
1.3×10^{-5}	0.00071
O_2	0.21
H_2O	0.217
N_2	0.5722

$$H_2 + \tfrac{1}{2}O_2 = H_2O$$

$$k_{\text{global}} = 1.8 \times 10^{13} \exp(-17614/T)[H_2]^{1.0}[O_2]^{0.5}$$

For the time being, this scheme does not include the effects of the small quantities of radicals present in the vitiated air. However, the assumption of a one-step mechanism instead of a more detailed mechanism can be justified based on the flame regime discussion in Sec. IV. In fact, CHEMKIN version 3.7 0-D simulations of H_2/air combustion with a detailed mechanism (9 species and 20 reactions) predicted ignition delay times of ~0.05 ms, which is 10 times shorter than the mixing time extracted from the experiments.

VI. Numerical Simulation Results

Numerical simulations with the ISCM model have already shown results in good agreement with the SCHOLAR data (see [30]). Two counter-rotating vortices are seen moving streamwise and straining the H_2 jet, confirming what was said about vorticity in Sec. III. The flame anchors at 5 cm from the injector and reaches the combustor exit, as in the experiments. The *instantaneous* temperature peaks (with the novel model for variable Sc_t of [30]) is ~2350 K, Temperature fluctuations are typically ~5%. Complex shock-boundary layer interaction and shock reflection extend upstream of the backward-facing step (see [23–30] for details). Temperature predictions were compared with experimental results and also with those by Keistler [71], who simulated the same test case with detailed chemistry (see Fig. 10).

Figure 10 shows temperature at $y = 18.2$ mm (near the bottom wall) at station 6 in Fig. 8. The black points are experimental, the black line is from [72], and the pink points are obtained with the ISCM model. Note that in [72] the number of grid points is about a factor 5 larger than in the present simulation. Figure 11 shows the pressure distribution along the centerline of the bottom wall: the pink line is for the ISCM model; the red and blue lines are, respectively, for the Connaire [73] and Jachimowski [74] kinetic schemes by Keistler [71]; and the broken line is for experiments. Figure 11 shows that the ISCM model (pink) predictions lie within the experimental scatter.

Experimental pressure peaks are 110,000 Pa at $X = 0.08$, 0.2, 0.45, and 0.6. Minimum pressure is ~100, 000 Pa at the exit of the (divergent) combustor. With the ISCM model, the trend and magnitude of pressure are the same, but the second peak is overpredicted. The last peak is 95,000 Pa at $X = 0.65$, whereas experiments show 110,000 Pa at $X = 0.6$. Simulations from [71] using Jachimowski's [74] H_2/air scheme and the Connaire et al. [73] scheme predict 65,000 Pa at the exit with both: that is, much less than in the experiment and less than predicted in this work (80,000 Pa). The reason for the pressure discrepancies is still being investigated but seems related to the slower-than-measured flame spreading.

Leaving aside the numerical differences, this comparison confirms that detailed chemical kinetics are not crucial to predict temperature in the flame region *in this particular test case*, because combustion is mixing-controlled here. These results also confirm that fast mixing and stable flame anchoring are indeed feasible.

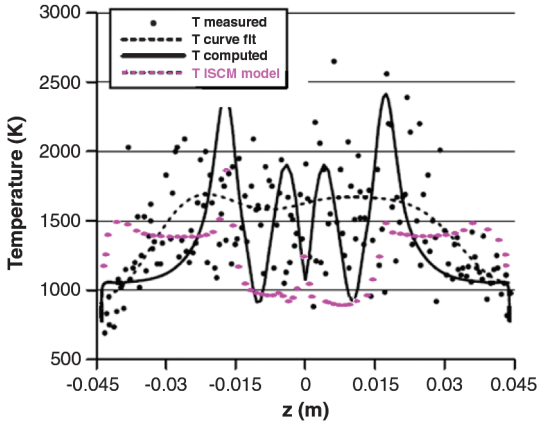

Fig. 10 Temperature slice of station 6 at $y = 18.2$ mm.

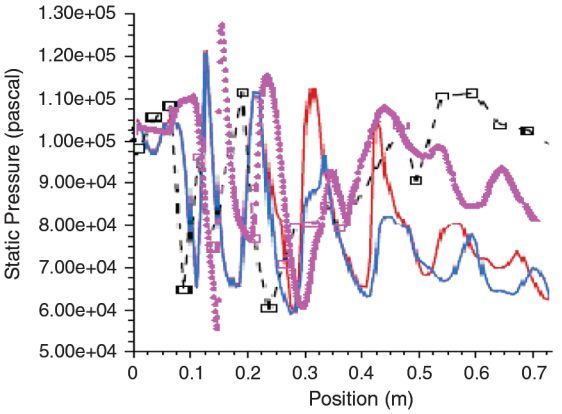

Fig. 11 Comparison of pressure distribution along centerline of bottom wall obtained with the ISCM model (pink line), Connaire [73] kinetic sheme results by Keistler [71] (red), Jachimowski [74] kinetic sheme results by Keistler [71] (blue), and experiments (broken line).

VII. Conclusions

The effects of Mach number and compressibility on turbulence and combustion have been theoretically analyzed. This study shows that supersonic internal flows that are representative of SCRJ combustors experience mainly streamwise vorticity and, consequently, maximum helicity: both tend to increase mixing, due to baroclinic and dilatational effects on turbulent KE decay. In particular, the KE slope in the inertial range is steeper and energy starts to be dissipated at lower wave numbers than in incompressible flows. One consequence is that dissipative eddies are larger in supersonic flows. A second consequence is in the combustion regime: in fact, in SC flames, the smallest eddies may be larger than the flame thickness and can only wrinkle the flame without entering it. This impacts the choice of model for the interaction between chemistry and

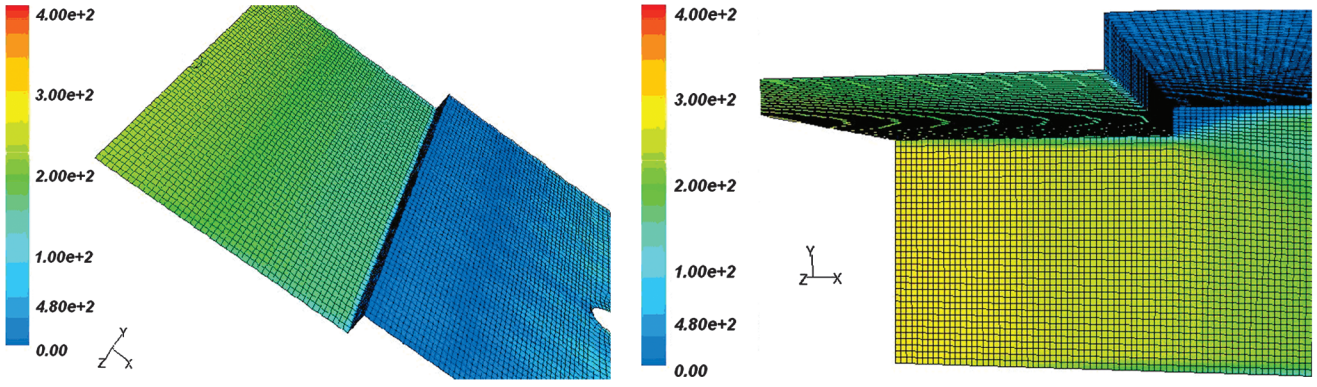

Fig. 9 Instantaneous contour of wall Y^+ at the combustor inlet upper wall.

turbulence, resulting in flame regimes that may differ from those in subsonic combustion, depending not only on Reynolds but also on the Mach number.

This physical modeling has been implemented in an LES CFD code and tested using experimental data. The LES reported in this paper indicates that SC occurs in the flamelets-in-eddies regime and reasonably well predicts flame anchoring, temperatures, and the pressure distribution, lending further support to the theoretical analysis performed.

As a more general conclusion, these results indicate that the physics of SC is complex and must be accommodated in CFD codes, starting as much as possible from fundamentals. Adapting or empirically modifying existing incompressible models is but a partial way of dealing with practical applications of SC and does not clarify its fundamental aspects.

Acknowledgments

This work was partly funded by the Long-Term Advanced Propulsion Concepts and Technologies (LAPCAT) project investigating high-speed airbreathing propulsion. LAPCAT, supervised by ESA European Space Research and Technology Centre, was supported by the European Union within the Sixth Framework Programme, Priority 1.4, Aeronautics and Space, contract no. AST4-CT-2005-012282. The authors also want to thank Paul A. Czysz, formerly at St. Louis University, for his steady support and for all the technical discussions they had with him over many years.

References

[1] Ladeinde, F., Cai, X., and Alabi, A., "A Critical Review of Scramjet Combustion Simulation," 47th AIAA Aerospace Sciences Meeting, AIAA Paper 2009-127, Orlando, FL, Jan. 2009.

[2] Christopher, J. R., and Frederick, G. B., "Review and Assessment of Turbulence Models for Hypersonic Flows: 2D/Axisymmetric Cases," 44th AIAA Aerospace Sciences Meeting, AIAA Paper 2006-713, Reno, NV, 9–12 Jan. 2006.

[3] Ferri, A., "Possible Direction of Future Research in Air Breathing Engines," *Fourth AGARD Combustion and Propulsion Colloquium*, Pergamon, London, 1961, pp. 3–15.

[4] Hallion, R. P., "The History of Hypersonics: Or, 'Back to the Future—Again and Again'," AIAA Paper 2005-329, Reno, NV, 10–13 Jan. 2005.

[5] Fry, R. S., "A Century of Ramjet Propulsion Technology Evolution," *Journal of Propulsion and Power*, Vol. 20, No. 1, 2004, pp. 27–58. doi:10.2514/1.9178

[6] Billig, F. S., "Research on Supersonic Combustion," *Journal of Propulsion and Power*, Vol. 9, No. 4, July–Aug. 1993, pp. 499–520. doi:10.2514/3.23652

[7] Mehta, U., "Hypersonic Technologies and Aerospace Plane," *Aerospace America*, Vol. 12, Dec. 2008, pp. 110–111.

[8] Swithenbank, J., Eames, I. W., Chin, S. B., Ewan, B. C. R., Yang, Z., Cao, J., and Zhao, X., "Turbulent Mixing in Supersonic Combustion," *High Speed Flight Propulsion Systems*, Progress in Astronautics and Aeronautics, Vol. 137, edited by S. N. B. Murthy, and E. T. Curran, AIAA, Reston, VA, 1991, pp. 341–382.

[9] Czysz, P., and Murthy, S. N. B., *Energy Management and Vehicle Synthesis*, Progress in Astronautics and Aeronautics, Vol. 165, AIAA, Reston, VA, 1996, pp. 581–686.

[10] Builder, C. H., "On the Thermodynamic Spectrum of Airbreathing Engines," AIAA Paper 64-243, 1964.

[11] Riggins, D. W., and McClinton, C. R., "Thrust Modelling for Hypersonic Engines," AIAA Paper 95-6081, 1995.

[12] Payne, R., "Supersonic Combustion of Liquid Kerosine," Ph.D. Dissertation, Univ. of Sheffield, Sheffield, England, U.K., 1975.

[13] *LAPCAT: Long-Term Advanced Propulsion Concepts and Technologies*, European Commission, http://ec.europa.eu/research/transport/projects/article_3666_en.html [retrieved Nov. 2009].

[14] Swithenbank, J., and Chigier, N. A., "Vortex Mixing for Supersonic Combustion," *21st (International) Symposium on Combustion*, Combustion Inst., Pittsburgh, PA, 1969. pp. 1154–62.

[15] Stalker, R. J., Paull, A., Mee, D. J., Morgan, R. G., and Jacobs, P. A., "Scramjets and Shock Tunnels—The Queensland Experience," *Progress in Aerospace Sciences*, Vol. 41, No. 6, 2005, pp. 471–513. doi:10.1016/j.paerosci.2005.08.002

[16] Ferri, A., "Mixing-Controlled Supersonic Combustion," *Annual Review of Fluid Mechanics*, Vol. 5, 1973, pp. 301–338. doi:10.1146/annurev.fl.05.010173.001505

[17] Swithenbank, J., "Flame Stabilization in High Velocity Flow," *Combustion Technology*, edited by H. Palmer, and J. M. Beer, Academic Press, NY, 1974, pp. 91–127.

[18] Portz, R., and Segal, C., "Penetration of Gaseous Jets in Supersonic Flows," 44th AIAA Aerospace Sciences Meeting, AIAA Paper 2006-1229, Reno, NV, 9–12 Jan. 2006.

[19] Czysz, P., "The High Temperature Hypersonic Gasdynamics Facility—Mach Number 4 Operation," Aeronautical Systems Div., Rept. ASD-TDR-63-236, Wright-Patterson AFB, OH, May 1963.

[20] Papamoschou, D., and Roshko, A.,"The Turbulent Compressible Shear Layer: An Experimental Study," *Journal of Fluid Mechanics*, Vol. 197, 1988, pp. 453–477. doi:10.1017/S0022112088003325

[21] Papamoschou, D.,"Effect of Three-Dimensionality on Compressible Mixing," *Journal of Propulsion and Power*, Vol. 8, No. 1, 1992, pp. 247–249. doi:10.2514/3.23467

[22] Papamoschou, D., and Bunyajitradulya, A.,"Evolution of Large Eddies in Compressible Shear Layers," *Physics of Fluids*, Vol. 9, No. 3, 1997, pp. 756–765. doi:10.1063/1.869230

[23] Ingenito, A., De Flora, G., Giacomazzi, E., Bruno, C., and Steelant, J., "LES Modeling of Scramjet Combustion," 44th AIAA Aerospace Sciences Meeting, AIAA Paper 2006-1383, Reno, NV, 9–12 Jan. 2006.

[24] Ingenito, A., De Flora, G., Giacomazzi, E., Bruno, C., and Steelant, J., "A Novel Model of Turbulent Supersonic Combustion: Development and Validation," 42nd AIAA/ASME/SAE/ASEE Joint Propulsion Conf., AIAA Paper 2006-4351, Sacramento, CA, 9–12 July 2006.

[25] Ingenito, A., Giacomazzi, E., Bruno, C., and Steelant, J., "Supersonic Combustion: Modelling and Simulations," 14th AIAA/AHI Space Planes and Hypersonic Systems and Technologies Conf., AIAA Paper 2006-7962, Canberra, Australia, 6–9 Nov. 2006.

[26] Ingenito, A., Bruno, C., and Steelant, J., "Advance in Supersonic Combustion Modeling and Simulations," 45th AIAA Aerospace Sciences Meeting, AIAA Paper 2007-837, Reno, NV, 8–11 Jan. 2007.

[27] Ingenito, A., and Bruno, C., "Advance in LES Modelling: Effect of the Turbulent Schmidt Number on Supersonic Regime," 43rd AIAA/ASME/SAE/ASEE Joint Propulsion Conf., AIAA Paper 2007-5633, Cincinnati, OH, 8–11 July 2007.

[28] Ingenito, A., and Bruno, C.,"Supersonic Mixing and Combustion: Advance in LES Modelling," *Advances in Aerospace Sciences-Propulsion Physics*, EUCASS Book Series, Vol. 1, edited by L. T. DeLuca, C. Bonnal, O. Haidn, and S. M. Frolov, Torus, Moscow, July 2007, pp. 471–486.

[29] Ingenito, A., and Bruno, C., "LES of a Supersonic Combustor with Variable Turbulent Prandtl and Schmidt Numbers," 46th AIAA Aerospace Sciences Meeting and Exhibit, AIAA Paper 2008-515, Reno, NV, 7–11 Jan. 2008.

[30] Ingenito, A., and Bruno, C., "LES of Supersonic Combustion with a Variable Turbulent Schmidt Number," 15th AIAA International Space Planes and Hypersonic Systems and Technologies Conf., AIAA Paper 2008-2586, Dayton, OH, 2008.

[31] Nishioka, M., Sakaue, S., Komada, K., Sakoshi, H., and Furukawa, I., "Mixing Transition in Supersonic Streamwise Vortices," *IUTAM Symposium on Elementary Vortices and Coherent Structures: Significance in Turbulence Dynamics*, Fluid Mechanics and Its Applications, Vol. 79, Springer, Amsterdam, 2006, pp. 249–258.

[32] Nishioka, M., Hiejima, T., Sunami, T., and Sakaue, S., "Streamwise Vortices as a Powerful Means for Supersonic Mixing Enhancement," *Proceedings of the International Symposium on Dynamics and Statics of Coherent Structures in Turbulence: Roles of Elementary Vortices*, edited by S. Kida, Springer, Amsterdam, 2002, pp. 217–228.

[33] Sunami, T., Wendt, M., and Nishioka, M., "Supersonic Mixing and Combustion Control Using Streamwise Vorticity," AIAA Paper 98-3271, 1998.

[34] Sunami, T., Itoh, K., Komuro, T., and Sato, K., "Effects of Streamwise Vortices on Scramjet Combustion at Mach 8–15," International Symposium on Airbreathing Engines, Paper 2005-1028, 2005.

[35] Fernando, E. M., and Menon, S., "Mixing Enhancement in Compressible Mixing Layers: An Experimental Study," *AIAA Journal*, Vol. 31, No. 2, 1993, pp. 278–285. doi:10.2514/3.11665

[36] Fox, J. S., Gastony, M. J., Houwing, A. F. P., and Danehy, P. M., "Comparison of Hypermixing Injectors Using a Mixture-Fraction-Sensitive Imaging Technique," *Proceedings of the 13th Australasian Fluid Mechanics Conference*, Monash Univ., Melbourne, Australia, 1998, pp. 79–82.

[37] Gutmark, E. J., Schadow, K. C., and Yu, K. H., "Mixing Enhancement in a Supersonic Free Shear Flows," *Annual Review of Fluid Mechanics*, Vol. 27, 1995, pp. 375–417. doi:10.1146/annurev.fl.27.010195.002111

[38] Thurow, B., Samimy, M., and Lempert, W., "Compressibility Effects on Turbulence Structures of Axisymmetric Mixing Layers," *Physics of Fluids*, Vol. 15, No. 6, 2003, pp. 1755–1765. doi:10.1063/1.1570829

[39] Friedrich, R., "Compressible Turbulent Flows: Aspects of Prediction and Analysis," *Applied Mathematics and Mechanics (ZAMM)*, Vol. 87, No. 3, 2007, pp. 189–211. doi:10.1002/zamm.200610312

[40] Marzouk, Y. M., and Ghoniem, A. F., "Mechanism of Streamwise Vorticity Formation in Transverse Jets," 40th AIAA Aerospace Sciences Meeting and Exhibit, AIAA Paper 2002-1063, Reno, NV, Jan. 2002.

[41] Kritsuk, A. G., Padoan, P., Wagner, R., and Norman, M. L., "Scaling Laws and Intermittency in Highly Compressible Turbulence," *AIP Conference Proceedings*, Vol. 932, American Inst. of Physics, Melville, NY, 2007, pp. 393–399.

[42] Kritsuk, A., Norman, M., Padoan, P., and Wagner, R., "The Statistics of Supersonic Isothermal Turbulence," *The Astrophysical Journal*, Vol. 665, No. 1, 2007, pp. 416–431. doi:10.1086/519443

[43] Gerlinger, P., Stollb, P., Kindler, M., Schneider, F., and Aigner, M., "Numerical Investigation of Mixing and Combustion Enhancement In Supersonic Combustors by Strut Induced Streamwise Vorticity," *Aerospace Science and Technology*, Vol. 12, No. 2, 2008, pp. 159–168. doi:10.1016/j.ast.2007.04.003

[44] Schetz, J. A., Maddalena, L., and Throckmorton, R., "Complex Wall Injector Array for High-Speed Combustors," *Journal of Propulsion and Power*, Vol. 24, No. 4, 2008, pp. 673–680. doi:10.2514/1.36660

[45] Hartfield, R. J., Hollo, S. D., and McDaniel, J. C., "Experimental Investigation of a Supersonic Swept Ramp Injector Using Laser Induced Iodine Fluorescence," *Journal of Propulsion and Power*, Vol. 10, No. 1, Jan.–Feb. 1994, pp. 129–135. doi:10.2514/3.23721

[46] Doerner, S. E., and Cutler, A. D., "Effects of Jet Swirl on Mixing of a Light Gas Jet in a Supersonic Airstream," NASA CR-1999-209842, Dec. 1999.

[47] Schetz, J. A., Cox-Stouffer, S., and Fuller, R., "Integrated CFD and Experimental Studies of Complex Injectors in Supersonic Flows," AIAA Paper 98-2780, June 1998.

[48] Riggins, D. W., and Vitt, P. H., "Vortex Generation and Mixing in Three-Dimensional Supersonic Combustors," *Journal of Propulsion and Power*, Vol. 11, No. 3, May–June 1995, pp. 419–426. doi:10.2514/3.23860

[49] Drummond, J. P., Carpenter, M. H., and Riggins, D. W., "Mixing and Mixing Enhancement in Supersonic Reacting Flowfields," *High Speed Flight Propulsion Systems*, edited by S. N. B. Murthy, and E. T. Curran, Progress in Astronautics and Aeronautics Series, Vol. 137, AIAA, Reston, VA, 1991, pp. 383–455.

[50] Rogers, R. C., "A Study of the Mixing of Hydrogen Injected Normal to a Supersonic Airstream," NASA Langley Research Center TN L-7386, Hampton, VA, 1971.

[51] Dimotakis, P. E., "On the Convection Velocity of Turbulent Structures in Supersonic Shear Layers," AIAA Paper 91-1724, 1991.

[52] Cutler, A. D., and Johnson, C. H., "The Use of Swirling Jet Pairs to Provide Rapid Fuel Penetration in Scramjet Combustors," AIAA Paper 95-0099, 1995.

[53] Kida, S., and Orszag, S. A., "Entropy Budget in Decaying Compressible Turbulence," *Journal of Scientific Computing*, Vol. 5, No. 1, 1990, pp. 1–34. doi:10.1007/BF01063424

[54] Kida, S., and Orszag, S., "Energy and Spectral Dynamics in Decaying Compressible Turbulence," *Journal of Scientific Computing*, Vol. 7, No. 1, 1992, pp. 1–34. doi:10.1007/BF01060209

[55] Biagioni, L., and D'Agostino, L.,"Measurement of Energy Spectra in Weakly Compressible Turbulence," 30th AIAA Fluid Dynamics Conf., AIAA Paper 99-3516, Norfolk, VA, 1999.

[56] Shapiro, A. H., *The Dynamics and Thermodynamics of Compressible Flow*, Ronald Press, New York, 1953, p. 228.

[57] Bellenoue, M., "Etude Experimentale de la Combustion Initiee par Effet Catalytique d'un Melange Hydrogene-Air en Ecoulement Supersonique," Ph.D. Dissertation, Univ. of Poitiers, Poitiers, France, Jan. 1997.

[58] Dimotakis, P. E.,"Turbulent Mixing," *Annual Review of Fluid Mechanics*, Vol. 37, 2005, pp. 329–356. doi:10.1146/annurev.fluid.36.050802.122015

[59] Ben-Yakar, A., Mungal, M. G., and Hanson, R. K., "Time Evolution and Mixing Characteristics of Hydrogen and Ethylene Transverse Jets in Supersonic Crossflows," *Physics of Fluids*, Vol. 18, No. 2, 2006, Paper 026101. doi:10.1063/1.2139684

[60] Moin, P., and Mahesh, K., "Direct Numerical Simulation: A Tool in Turbulence Research," *Annual Review of Fluid Mechanics*, Vol. 30, 1998, pp. 539–78.

[61] Pirozzoli, S., and Grasso, F., "Direct Numerical Simulations of Isotropic Compressible Turbulence: Influence of Compressibility on Dynamics and Structures," *Physics of Fluids*, Vol. 16, No. 12, Dec. 2004, pp. 4386–4407. doi:10.1063/1.1804553

[62] Moelwyn-Hughes, E. A., *Physical Chemistry*, Pergamon, London, 1965, pp. 45–50.

[63] Park, C., *Nonequilibrium Hypersonic Aerothermodynamics*, Wiley, New York, 1989, pp. 119–142.

[64] Giordano, D., "The Influence of Medium Comprimibility on Chemical-Reaction Rates, Part 1: Theoretical Considerations," 36th AIAA Thermophysics Conf., AIAA Paper 2003-4057, Orlando, FL, 23–26 June 2003.

[65] Gerasimov, G. Y., and Kolesnichenko, G., "Transport Phenomena in a Nonequilibrium Dissociative Gas," *Fluid Dynamics*, Plenum, Moscow, 1984, pp. 794–800.

[66] Makashev, N. K., "The Effect Of Gas Motion On The Reaction Kinetics of the Vibrationally Excited Molecules," *Fluid Dynamics*, Plenum, Moscow, 1985, pp. 943–949.

[67] Makashev, N. K., "Nonequilibrium Dissociation of Diatomic Molecules in Flows with Convective and Diffusive Particle Transport," *Fluid Dynamics*, Vol. 19, Plenum, Moscow, 1985, pp. 957–963.

[68] Bray, K. N. C., Libby, P. A., and Williams, F. A., "High Speed Turbulent Combustion," *Turbulent Reacting Flows*, Academic Press, London, 1994, pp. 609–638.

[69] Magnussen, B. F., "The Eddy Dissipation Concept for Turbulent Combustion Modeling. Its Physical and Practical Implications," Div. of Thermodynamics, Norwegian Inst. of Technology, Rept. N-7034, Throndheim, Norway, Oct. 1989.

[70] Marinov, N. M., Westbrook, C. K., and Pitz, W. J., "Detailed and Global Chemical Kinetics Model for Hydrogen," *Transport Phenomena in Combustion*, Vol. 1, Taylor and Francis, Washington, D.C., 1996, pp. 118–129.

[71] Kiestler, P. G., "Simulation of Supersonic Combustion Using Variable Turbulent Prandtl/Schmidt Numbers Formulation," Ph.D. Dissertation, Aerospace Engineering Dept., North Carolina Univ., Raleigh, NC, 2007.

[72] Choi, J. Y., and Yang, V., "Combustion Oscillations in a Scramjet Engine Combustor with Transverse Fuel Injection," *Proceedings of the 30th Symposium (International) on Combustion*, Vol. 30, Combustion Inst., Pittsburgh, PA, 2005, pp. 2851–2858.

[73] Connaire, M. O., Curran, H. J., Simmie, J. M., Pitz, W. J., and Westbrook, C. K., "A Comprehensive Modeling Study of Hydrogen Oxidation," *International Journal of Chemical Kinetics*, Vol. 36, No. 11, 2004, pp. 603–622. doi:10.1002/kin.20036

[74] Jachimowski, C. J., "An Analytic Study of the Hydrogen-Air Reaction Mechanism with Application to Scramjet Combustion," NASA TR 2781, Feb. 1988.

F. Ladeinde
Associate Editor